Development 137, 2095-2105 (2010) doi:10.1242/dev.049494

Distinct functions of BMP4 during different stages of mouse ES cell neural commitment

Kejing Zhang[1,*], Lingyu Li[1,*], Chengyang Huang[1], Chengyong Shen[1], Fangzhi Tan[1], Caihong Xia[1], Pingyu Liu[1], Janet Rossant[2] and Naihe Jing[1,†]

SUMMARY

Bone morphogenetic protein (BMP) signaling plays a crucial role in maintaining the pluripotency of mouse embryonic stem cells (ESCs) and has negative effects on ESC neural differentiation. However, it remains unclear when and how BMP signaling executes those different functions during neural commitment. Here, we show that a BMP4-sensitive window exists during ESC neural differentiation. Cells at this specific period correspond to the egg cylinder stage epiblast and can be maintained as ESC-derived epiblast stem cells (ESD-EpiSCs), which have the same characteristics as EpiSCs derived from mouse embryos. We propose that ESC neural differentiation occurs in two stages: first from ESCs to ESD-EpiSCs and then from ESD-EpiSCs to neural precursor cells (NPCs). We further show that BMP4 inhibits the conversion of ESCs into ESD-EpiSCs during the first stage, and suppresses ESD-EpiSC neural commitment and promotes non-neural lineage differentiation during the second stage. Mechanistic studies show that BMP4 inhibits FGF/ERK activity at the first stage but not at the second stage; and IDs, as important downstream genes of BMP signaling, partially substitute for BMP4 functions at both stages. We conclude that BMP signaling has distinct functions during different stages of ESC neural commitment.

KEY WORDS: Embryonic stem cells, Epiblasts, EpiSCs, BMP4, Neural commitment, Mouse

INTRODUCTION

During mouse embryonic development, the embryonic day (E) 3.5 blastocyst becomes a vesicular structure comprising an inner cell mass (ICM) inside the trophectoderm (Gardner and Beddington, 1988). By the time of implantation (E4.0-E4.5), the pluripotent ICM cells differentiate to form the primitive endoderm and epiblast (Gardner and Rossant, 1979). From E4.5 to E5.5, the blastocyst gives rise to a cup-shaped structure called the egg cylinder, and the epiblast at this stage is composed of a columnar epithelial monolayer of pluripotent cells (Coucouvanis and Martin, 1995; Snow, 1977). Gastrulation then commences with the formation of the primitive streak at approximately E6.5, through which epiblast cells ingress to form the mesoderm and the endoderm. The cells that remain in the anterior of the epiblast form the ectoderm (Lu et al., 2001; Tam and Loebel, 2007). Neural induction is the process during which part of the ectoderm is specified and becomes the embryonic neural plate. This process is generally thought to occur at the onset of gastrulation (Hemmati-Brivanlou and Melton, 1997b). To date, knowledge of the molecular mechanisms governing these events in the mouse embryo is limited owing to the small size, complexity and inaccessibility of the early post-implantation embryo, and to the rapid pace of cell proliferation.

Mouse embryonic stem cells (ESCs) are immortal cell lines derived mainly from the ICM of peri-implantation blastocysts (Brook and Gardner, 1997; Evans and Kaufman, 1981; Martin, 1981). The lineage restriction of mouse ESCs is identical to that of the epiblast progenitors in the ICM, suggesting that ESCs might represent an in vitro model of early epiblast development (Rossant, 2008). However, recent evidence has shown that ESCs are not homogenous and appear to be in a metastable state, shifting between ICM- and epiblast-like states while remaining pluripotent (Chambers et al., 2007; Hayashi et al., 2008; Toyooka et al., 2008). Epiblast stem cells (EpiSCs) have been isolated from the epithelialized epiblast of mouse and rat egg cylinders (Brons et al., 2007; Tesar et al., 2007). EpiSCs can be maintained as stable cell lines in the presence of FGF and activin, and they are capable of differentiating into three germ layers in vitro and of forming teratomas. On the basis of their developmental potential, EpiSCs are believed to resemble pluripotent progenitors in the late epiblast layer of the post-implantation mouse embryo (Brons et al., 2007). However, it is unclear whether ESC neural differentiation in vitro recapitulates the different stages of the developmental process from the ICM to neuroectoderm in vivo (Rossant, 2008; Silva and Smith, 2008).

Bone morphogenetic proteins (BMPs) are members of the transforming growth factor β (TGFβ) superfamily (Shi and Massague, 2003). In the past decade, the default model has proposed that ectodermal cells give rise to neural tissue autonomously in the absence of inhibitory BMP signals, whereas BMP activity directs ectoderm to become epidermis (Hemmati-Brivanlou and Melton, 1997a). Although this default model has been challenged by studies in *Xenopus* and chick embryos (De Robertis and Kuroda, 2004; Linker and Stern, 2004; Wilson and Edlund, 2001), recent studies have shown that the complete inhibition of BMP signaling is sufficient to induce neural tissue (Di-Gregorio et al., 2007; Khokha et al., 2005; Reversade and De

[1]Laboratory of Molecular Cell Biology, Institute of Biochemistry and Cell Biology, Shanghai Institutes for Biological Sciences, Chinese Academy of Sciences, 320 Yue Yang Road, Shanghai 200031, China. [2]Program in Developmental and Stem Cell Biology, Hospital for Sick Children Research Institute, Department of Molecular Genetics, University of Toronto, 555 University Avenue, Toronto, ON M5G 1X8, Canada.

*These authors contributed equally to this work
†Author for correspondence (njing@sibs.ac.cn)

Accepted 23 April 2010

Robertis, 2005). In mouse ESCs, BMP signaling is crucial for maintaining pluripotency (Kawasaki et al., 2000; Tropepe et al., 2001; Ying et al., 2003a), and also has negative effects on neural differentiation (Kawasaki et al., 2000; Tropepe et al., 2001; Ying et al., 2003b). It has been reported that BMP4-induced ID proteins can inhibit ESC entry into the neural lineage, and can sustain ESC self-renewal in collaboration with LIF/STAT3 (Ying et al., 2003a). However, it remains unclear when and how BMP signaling regulates these different functions during ESC neural commitment.

Here, we show that there is a BMP4-sensitive window during mouse ESC neural commitment. Cells at this stage correspond to the epiblast of the egg cylinder, and can be maintained as ESC-derived EpiSCs (ESD-EpiSCs). We further show that BMP4 inhibits ESC neural differentiation in two phases: first, it inhibits the derivation of ESD-EpiSCs from mouse ESCs; and second, it suppresses the neural commitment of ESD-EpiSCs and promotes their non-neural differentiation.

MATERIALS AND METHODS

ESC culture and neural differentiation

Mouse ESC lines R1, R1/E (ATCC), E14Tg2a, SOX-GFP ES cells (46C), and TAU-GFP ES cells (TK23) (Ying et al., 2003b) were used in this study. ESCs were maintained on mitomycin C-treated mouse embryonic fibroblasts (MEFs; feeders) in standard medium. ESC neural differentiation was induced as described previously (Watanabe et al., 2005).

Derivation of ESD-EpiSCs and cell culture

For derivation of ESD-EpiSCs, ESC aggregates were dissociated into a single-cell suspension after 5 minutes of treatment with 0.05% Trypsin-EDTA at 37°C. Individual cells were then seeded at a density of 1.0-2.0×10^5 cells per 35-mm dish in chemically defined medium (CDM) (Brons et al., 2007) supplemented with 20 ng/ml activin A (R&D Systems) and 12 ng/ml bFGF (Invitrogen). The cell culture dish was coated with FBS for 24 hours at 37°C and then washed twice with PBS before use. After 5-6 days culture, the surviving cells grew and formed large compact colonies. The colonies were picked, fragmented into smaller clumps using 2 mg/ml collagenase IV (Invitrogen) and mechanical dissociation, and similarly passaged at 3-day intervals. Medium was changed every day. Detailed protocols for ESD-EpiSC culture and differentiation are available upon request.

Gene overexpression in ESCs and ESC-EpiSCs

For gene overexpression in ESCs (ESR1) and ESD-EpiSCs, mouse *Id1* and *Id2* full-length cDNAs were cloned into the lentiviral expression vector pFUGW-IRES-EGFP (Naldini et al., 1996). The empty lentiviral expression vector pFUGW-GFP was used as a negative control. Lentiviral packaging and lentiviral transfection were performed as described (Tiscornia et al., 2006). For ESCs, GFP-positive cells were sorted with a FACS Aria cell sorter (BD Biosciences), and for ESD-EpiSCs, GFP-positive colonies were selected by fluorescence microscopy.

Immunofluorescence analysis

Alkaline phosphatase staining was performed according to the manufacturer's instructions using the Alkaline Phosphatase (AKP) Detection Kit (Millipore). Immunocytochemistry was performed as described (Gao et al., 2001; Xia et al., 2007). The following primary antibodies were used. Mouse monoclonal antibodies included: anti-OCT4 (1:200, Santa Cruz Biotechnology), anti-nestin (1:200, Upstate), anti-SSEA-1 (1:200, Santa Cruz), anti-TUJ1 (1:500; Sigma), anti-SOX17 (10 μg/ml, R&D Systems), anti-nebulin (1:100, Sigma), and anti-cytokeratin 18 (1:100, Abcam). Rabbit polyclonal antibodies were anti-FGF5 (1:150; Santa Cruz) and an anti-SOX1/(2)/3 (1:100) that has a preference for SOX1 and SOX3 over SOX2 (Okada et al., 2004; Tanaka et al., 2004). Goat polyclonal antibodies were anti-NKX2.5 (1:200, Santa Cruz) and anti-GATA6 (10 μg/ml, R&D Systems).

RNA preparation and Q-PCR analysis

Total RNA was extracted from cells using Trizol reagent (Invitrogen). Reverse transcription and Q-PCR were performed as described previously (Peng et al., 2009). The primers used are listed in Table S1 in the supplementary material.

Microarray analysis

Total RNA was extracted using Trizol reagent, labeled, and hybridized to Agilent Whole Mouse Genome Oligo 4X44K Microarrays (one-color platform), according to the manufacturer's protocols. The comparison between mouse ESCs and ESD-EpiSCs was carried out using three biological replicates for each cell type. ESC samples (ESR1 p10, p20, and ESR1/E p15) and ESD-EpiSC samples (EpiSC-7 p20, EpiSC-5 p22, and EpiSC-7 p25) were used for microarray analysis. Microarray data has been deposited with ArrayExpress with the Accession Number E-MEXP-2691.

Statistical analyses

In each experiment, 100-200 cell aggregates were examined. Each experiment was performed at least three times. Values shown on the graphs represent the mean value ± s.d. Student's *t*-tests were used to compare the effects of all treatments. Statistically significant differences are shown as follows: $*P<0.05$, $**P<0.01$ and $***P<0.001$.

RESULTS

BMP4 suppresses neural differentiation of mouse ESCs

Many protocols have been developed to induce the differentiation of mouse ESCs into the neuroectodermal lineage (Bibel et al., 2004; Watanabe et al., 2005; Ying et al., 2003b). To avoid influences from feeder cells, growth factors and retinoic acid, we cultured embryoid bodies (EBs) in a medium supplemented with knockout serum replacement (KSR medium) for ESC neural conversion (Watanabe et al., 2005). Immunostaining showed that 98% of the non-induced ESCs were $OCT4^+/SOX^+$ undifferentiated pluripotent cells (Fig. 1Aa-c,B). During 8 days of culture in KSR medium, the number of $OCT4^+/SOX^+$ pluripotent cells decreased gradually (Fig. 1D), and the percentage of $OCT4^-/SOX^+$ cells reached approximately 80% of the total cells by day 6 (Fig. 1Ad-f,B,D). These $OCT4^-/SOX^+$ cells were putative neural precursor cells (NPCs) (Wood and Episkopou, 1999; Xia et al., 2007), and this was further confirmed by the presence of another NPC marker nestin (Lendahl et al., 1990) (see Fig. S1A in the supplementary material). In addition, we used ESC line 46C (Ying et al., 2003b), in which GFP was knocked in at the locus of the specific neuroectoderm marker gene *Sox1*, and FACS analysis showed that the number of SOX1-GFP^+ cells reached between 70 and 80% of the total cells at day 6 (see Fig. S1B in the supplementary material). When the day 6 EBs were replated onto serum-free N2 medium, these NPCs differentiated into $TUJ1^+$ neurons within 2 days (Fig. 1Ca-b); $MAP2^+$ neurons and $GFAP^+$ astrocytes could also be detected 4 days after replating (see Fig. S1C in the supplementary material). Together, these results show that a high proportion of ESCs can be converted into neural precursors in KSR medium.

Consistent with previous reports that BMP signaling has a negative effect on ESC neural differentiation (Kawasaki et al., 2000; Sasal et al., 1995; Wilson and Hemmati-Brivanlou, 1995; Ying et al., 2003b), the addition of BMP4 (10 ng/ml) greatly reduced the number of $OCT4^-/SOX^+$ NPCs in day 6 EBs (Fig. 1Ag-i), as well as the number of $TUJ1^+$ neurons after replating (Fig. 1Cc-d). Moreover, BMP4 was reported to maintain ESC pluripotency (Kawasaki et al., 2000; Ying et al., 2003a). We consistently found that approximately 50% of cells in the BMP4-treated EBs remained $OCT4^+/SOX^+$ (Fig. 1B), corresponding to putative pluripotent ESCs. To further confirm this notion, we

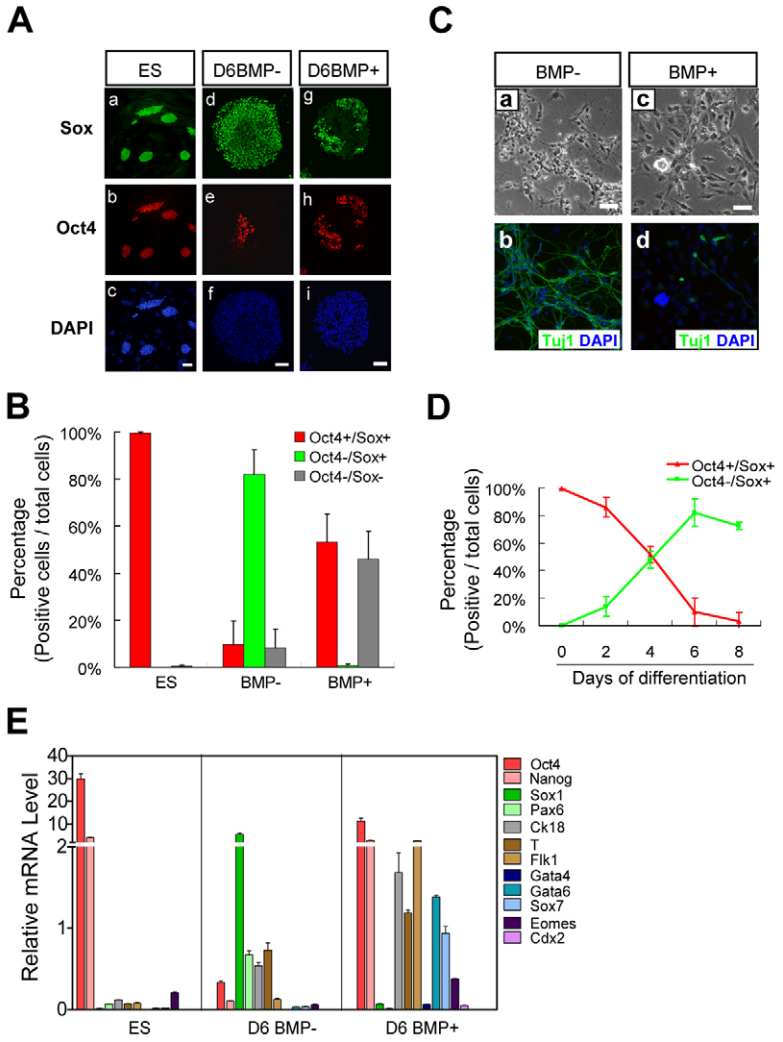

Fig. 1. Efficient mouse ESC neural commitment in KSR medium is inhibited by BMP4. (**A**) Double immunostaining for OCT4 and SOX proteins in undifferentiated ESCs (a-c), and in day 6 EBs cultured in KSR medium without (d-f) or with (g-i) BMP4 (10 ng/ml). Nuclei were stained with DAPI. Scale bar: 50 μm. (**B**) Percentages of OCT4$^+$/SOX$^+$, OCT4$^-$/SOX$^+$ and OCT4$^-$/SOX$^-$ cells obtained following culture under the above conditions. The results were obtained from three independent experiments. (**C**) EBs were cultured in KSR medium supplemented without (–) or with (+) BMP4 for 6 days and then replated into N2 medium for 2 days of adherent culture. Shown are images indicating cellular morphology (a,c), and immunostaining for class III tubulin (TUJ1) with DAPI staining (b,d). Scale bar: 50 μm. (**D**) Percentages of OCT4$^+$/SOX$^+$ and OCT4$^-$/SOX$^+$ cells during 8 days of ESC neural differentiation. (**E**) Q-PCR analysis for germ layer markers expressed in EBs following culture in KSR medium for 6 days. BMP4 was added to the medium (D6 BMP+) or was not added (D6 BMP–). Undifferentiated ESCs served as a negative control (ES). Relative gene expression levels were normalized to the expression of *Gapdh*.

replated day 6 EBs into ESC medium and found that the number of AKP-positive colonies derived from BMP4-treated EBs increased significantly (see Fig. S1D in the supplementary material). The remaining 50% of cells in the BMP4-treated EBs were OCT4$^-$/SOX$^-$ (Fig. 1B). To identify the cell lineages to which these OCT4$^-$/SOX$^-$ double-negative cells belonged, we examined the expression of three germ layer markers by Q-PCR and found that, in addition to the expression of the pluripotent markers *Oct4* and *Nanog*, BMP4-treated day 6 EBs also expressed a high level of epidermal (*CK18*; *Krt18* – Mouse Genome Informatics), mesodermal (*T*, *Flk1*), and primitive endodermal (*Gata6*, *Sox7*) markers, but expressed very low levels of neuroectoderm markers (*Sox1*, *Pax6*; Fig. 1E, right panel). Taken together, these data show that BMP4 inhibits ESCs neural differentiation in KSR medium by maintaining the pluripotency of a portion of the cells and by promoting others to differentiate into non-neural lineages.

Identification of a BMP4-sensitive window during ESC neural commitment

As maintaining ESC pluripotency and promoting cell differentiation are opposite functions, we assumed this effect might be associated with long-term BMP4 treatment. To determine whether short-term BMP4 treatment was sufficient to inhibit ESC neural differentiation, BMP4 was added to the KSR medium at different time points, and the cells were cultured in the presence of BMP4 for 24 hours. We defined the day on which the ESCs were seeded as differentiation day 0 and stained the EBs for OCT4 and SOX at day 6. The most significant suppression of neural differentiation was achieved when BMP4 was added during day 2-3, with only 11% of the cells developing into OCT4$^-$/SOX$^+$ NPCs and 72% becoming OCT4$^-$/SOX$^-$ non-neural cells (Fig. 2A,B, BMP4+, 2-3). By contrast, the addition of BMP4 at other time points was less effective at inhibiting ESC neural differentiation (Fig. 2A,B). These results suggest that ESCs are most sensitive to BMP4-mediated inhibition of neural differentiation on the second or third differentiation day.

To determine whether the absence of BMP4 was sufficient to specify neural fate during the BMP4-sensitive window, we cultured EBs in BMP4-containing KSR medium and then withdrew BMP4 from the medium for 2 days at different periods of differentiation. The highest number of OCT4$^-$/SOX$^+$ NPCs was obtained when BMP4 was withdrawn during days 2-4 of the induction period (see Fig. S2 in the supplementary material, BMP4+, 0-2, 4-6). We also noticed that the addition of BMP4 did not maintain OCT4$^+$/SOX$^+$ pluripotent cells after day 2 (see Fig. S2 in the supplementary material, BMP4+, 2-6). To further confirm this observation, we cultured EBs in KSR medium for different numbers of days and added BMP4 until day 6. Before day 2, the addition of BMP4 maintained the OCT4$^+$/SOX$^+$ pluripotent cells (Fig. 2C,D). At day 2, the addition of BMP4 primarily promoted the differentiation of

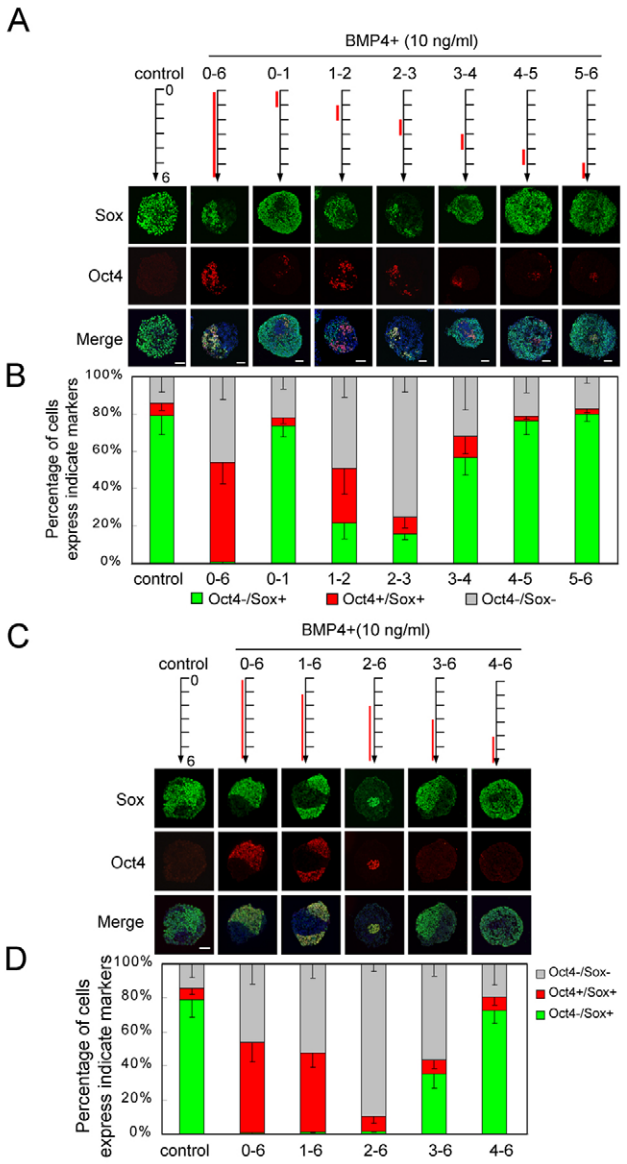

Fig. 2. Window of ESC responsiveness to BMP4 inhibition during neural commitment. (**A**) Double immunostaining for OCT4 and SOX in EBs cultured in KSR medium for 6 days. Nuclei were stained with DAPI. BMP4 (10 ng/ml) was added to the medium on the indicated days (red lines). Scale bar: 50 μm. (**B**) Percentage of OCT4$^+$/SOX$^+$ (red), OCT4$^-$/SOX$^+$ (green) and OCT4$^-$/SOX$^-$ (gray) cells obtained following culture under the conditions described in A. (**C**) Double immunostaining for OCT4 and SOX in EBs cultured in KSR medium for 6 days. Nuclei were stained with DAPI. BMP4 was added to the medium on the indicated day (red line). Scale bar: 50 μm. (**D**) Percentages of OCT4$^+$/SOX$^+$, OCT4$^-$/SOX$^+$ and OCT4$^-$/SOX$^-$ cells obtained following culture under the conditions described in C.

ESCs into OCT4$^-$/SOX$^-$ cells (Fig. 2A,B). However, after day 3, BMP4 addition only slightly inhibited ESC neural differentiation (Fig. 2C,D). In contrast to a previous study (Gambaro et al., 2006), we found that BMP4 did not significantly increase the number of apoptotic cells (data not shown), which might due to different culture conditions. These results suggest that once neural differentiation is initiated, BMP4 cannot inhibit it. Therefore, the BMP4-sensitive window appears to be a crucial time during which BMP4 switches its function from maintaining ESC pluripotency to promoting non-neural lineage differentiation.

Cells at the BMP4-sensitive window are similar to egg cylinder-stage epiblast cells

Because ESC differentiation in vitro might recapitulate the process of embryonic development in vivo (Rathjen et al., 1999), we wondered to which in vivo developmental stage the BMP4-sensitive cells correspond. To address this question, we examined gene expression patterns during ESC EB differentiation in KSR medium (Fig. 3A), and found that the genes most commonly used as ICM markers, including *Rex1*, *Crtr-1* (*Tcfcp2l1* – Mouse Genome Informatics) and *Fgf4* (Nichols et al., 1998; Pelton et al., 2002; Rogers et al., 1991), were expressed from day 0-1, and rapidly downregulated after day 2. The pluripotent stem cell marker *Oct4* (Rosner et al., 1990) was expressed highly from days 0 to 3, and was then downregulated (Fig. 3Aa,b). *Fgf5*, a marker of pluripotent epiblast cells (Haub and Goldfarb, 1991; Rathjen et al., 1999), was transiently upregulated on day 2-3, followed by a peak expression of *T* (brachyury) at day 4. *T* is a primitive streak marker that marks the beginning of gastrulation (Rivera-Perez and Magnuson, 2005; Tam and Loebel, 2007) (Fig. 3Ab). Markers of neuroectoderm were expressed later: the anterior ectodermal marker *Hesx1* was expressed highly at day 5, followed by the specific neural marker *Sox1* (peak expression at day 6) and the anterior neural plate marker *Six3* (expressed by day 8) (Oliver et al., 1995; Pevny et al., 1998; Thomas and Beddington, 1996) (Fig. 3Ac). A detailed comparison of these expression patterns suggests that ESC neural differentiation closely mimics early embryonic development in vivo (Pfister et al., 2007), and that cells at the BMP4-sensitive window (day 2-3) are similar to cells of the epiblast of egg cylinder stage (Fig. 3B). To further confirm this observation, we compared the expression levels of ESC- and EpiSC-related genes (Tesar et al., 2007; Toyooka et al., 2008) in day 2 EBs and undifferentiated ESCs. Day 2 EBs expressed lower levels of genes associated with the ICM or blastocyte epiblasts, such as *Klf4*, *Tbx3*, *Rex1* and *Nanog*, but strongly expressed the egg-cylinder-stage epiblast-associated genes *Pitx2*, *Fgf5*, *Cer1* and *Foxa2* (Fig. 3C). These results strongly suggest that EB cells at day 2-3 are comparable to cells of the egg-cylinder-stage epiblast.

ESD-EpiSCs have the same characteristics as EpiSCs derived from mouse embryos

Because the cells in day 2-3 EBs were similar to egg cylinder epiblast cells, we sought to determine whether they could be maintained in a similar manner to EpiSCs in vitro. Because chemically defined medium containing activin A and bFGF (CDM/AF) is sufficient to maintain the pluripotency of EpiSCs derived from post-implantation mouse embryos (Brons et al., 2007), we dissociated the day 2 EBs into single-cell suspensions and seeded the cells in CDM/AF. After 6 days of culture, homogeneous and compact monolayer colonies formed, and the cells in these colonies showed a high nuclear-cytoplasmic ratio (Fig. 4A). Moreover, these cells could be propagated in the CDM/AF culture system for more than 50 passages without obvious changes (see Fig. S3 in the supplementary material). Immunostaining of the cells showed that they expressed the pluripotency markers OCT4 and SSEA-1 (Fut4 – Mouse Genome Informatics), and the epiblast cell marker FGF5, but the expression of AKP was much lower than in mouse ESCs (Fig. 4B). As determined by Q-PCR, these cells did not express the ESC marker

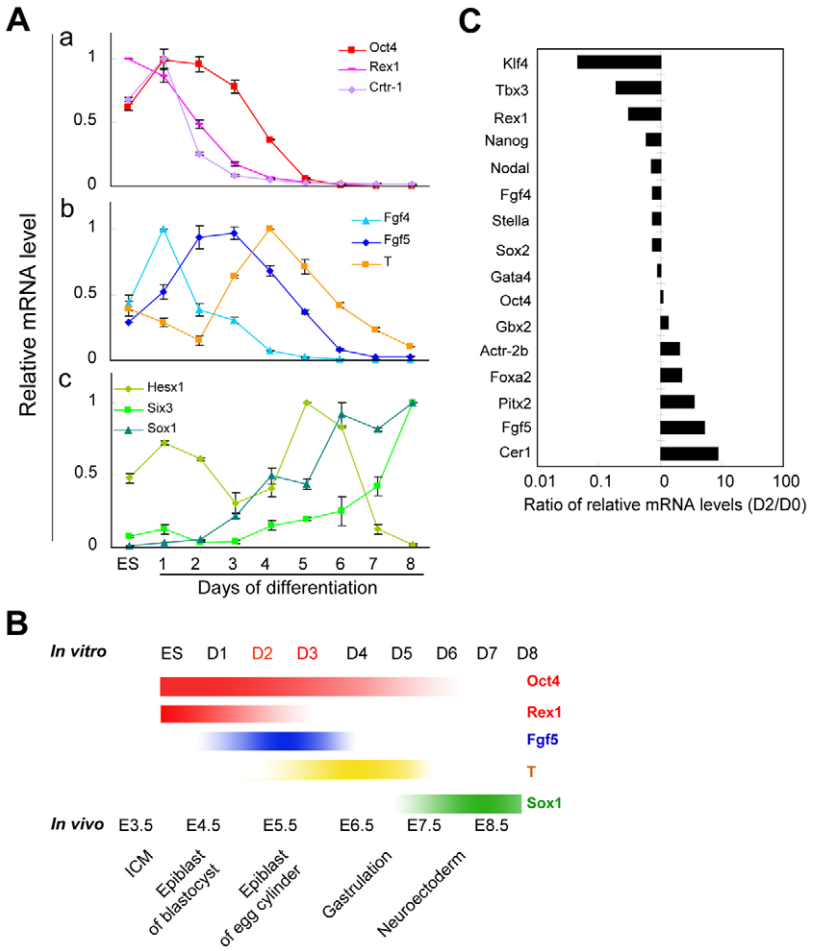

Fig. 3. The BMP4-sensitive window corresponds to the egg cylinder epiblast stage. (**A**) Q-PCR analysis of marker gene expression patterns during ESC neural differentiation from days 0-8. Three groups of marker genes were analyzed: the ICM markers *Rex1*, *Crtr-1* and *Fgf4* and the pluripotent marker *Oct4* (a,b); the epiblast marker *Fgf5* and the primitive streak marker *T* (b); and the neuroectoderm markers *Hesx1*, *Sox1* and *Six3* (c). Relative mRNA levels were determined by normalization to the expression of *Gapdh*. (**B**) Proposed model correlating ESC neural differentiation with the neural induction process in mouse embryos. The temporal expression pattern of marker genes in vitro is similar to the expression pattern of those genes in vivo, suggesting that the progeny of ESC differentiation in vitro can reflect the comparable states of cells in vivo. (**C**) Relative expression levels of ICM- or epiblast-associated genes in day 2 EBs (D2) and undifferentiated ESCs (D0) was examined by Q-PCR.

Rex1, but did express the post-implantation embryo markers *Nodal* and *Fgf5* (Fig. 4C). Relative to ESCs, these cells expressed lower levels of *Nanog* and *Sox2*, and a similar level of *Oct4* (Fig. 4C). Furthermore, these EpiSC-like cells could not convert back into ESCs when cultured in standard ESC medium (see Fig. S4A in the supplementary material). Collectively, these results suggest that the ESC-derived EpiSC-like cells (ESD-EpiSCs) have characteristics of EpiSCs and can be maintained as stable cell lines.

To determine whether ESD-EpiSCs can only be derived from day 2 EBs, we cultured EBs in KSR medium for 1-5 days. Each day, the EBs were dissociated into single-cell suspensions and the cells were seeded in CDM/AF medium at the same density. We found that EpiSC-like colonies could be obtained from day 1-5 EBs, as well as non-induced ESCs; the day 2 EBs gave the highest colony number (Fig. 4D). This suggests the accumulation of EpiSC-like cells in day 2 EBs.

To further characterize the ESD-EpiSCs, we used the formation of EBs and teratomas to examine the differentiation potential of ESD-EpiSCs. EB differentiation was achieved by growing small clumps of ESD-EpiSCs in KSR medium or DMEM medium containing 10% FBS. After 3 days of differentiation, markers of all three germ layers were expressed, including *Sox1* and *Ck18* (ectodermal), *Flk1*, *Mixl1* and *Sox17* (mesodermal), and *Gata4*, *Gata6* and *Sox7* (endodermal), as well as trophectodermal markers (*Cdx2, Dlx3* and *Hand1*) (Fig. 4E). Furthermore, TUJ1$^+$ neurons, CK18$^+$ epithelial cells, NKX2-5$^+$ cardiomyocytes, nebulin$^+$ skeletal myofibers and GATA6$^+$ endoderm-like cells were all observed in the differentiated outgrowth from ESD-EpiSC EBs (see Fig. S4B in the supplementary material). To examine the differentiation capacity of ESD-EpiSCs in vivo, we injected them into ectopic sites of immunodeficient mice and observed the formation of teratomas that contained a wide variety of tissue types, including neural epithelium, cartilage, adipocytes and gut (Fig. 4F). These data show that ESD-EpiSCs are capable of differentiating into derivatives of all three primary germ layers and into extra-embryonic tissues.

To further define the molecular properties of ESD-EpiSCs, we performed a microarray analysis to determine the transcriptional profile of ESD-EpiSCs and mouse ESCs. After comparing the data from EpiSCs and ESCs (Tesar et al., 2007), we selected the top 5000 differentially expressed genes for a cluster analysis, which showed that the ESD-EpiSCs were transcriptionally more similar to EpiSCs than to mouse ESCs (see Fig. S4C in the supplementary material). Several known ICM markers, including *Rex1* (*Zfp42*), *Dppa3* (*Stella*), *Tbx3* and *Klf4*, and the epiblast markers *Fgf5*, *Foxa2*, *Lefty1/2* and *Cer1*, were all included among these differentially expressed genes, and these genes had similar expression levels in ESD-EpiSCs and EpiSCs (Fig. 4G). Together, these data indicate that ESD-EpiSCs derived in vitro closely resemble EpiSCs from early mouse embryos.

BMP4 inhibits the derivation of ESD-EpiSCs from ESCs

Because ESD-EpiSCs could be obtained during ESC neural differentiation, it is reasonable to divide this process into two stages: the transition from ESCs to EpiSCs, and the transition from EpiSCs

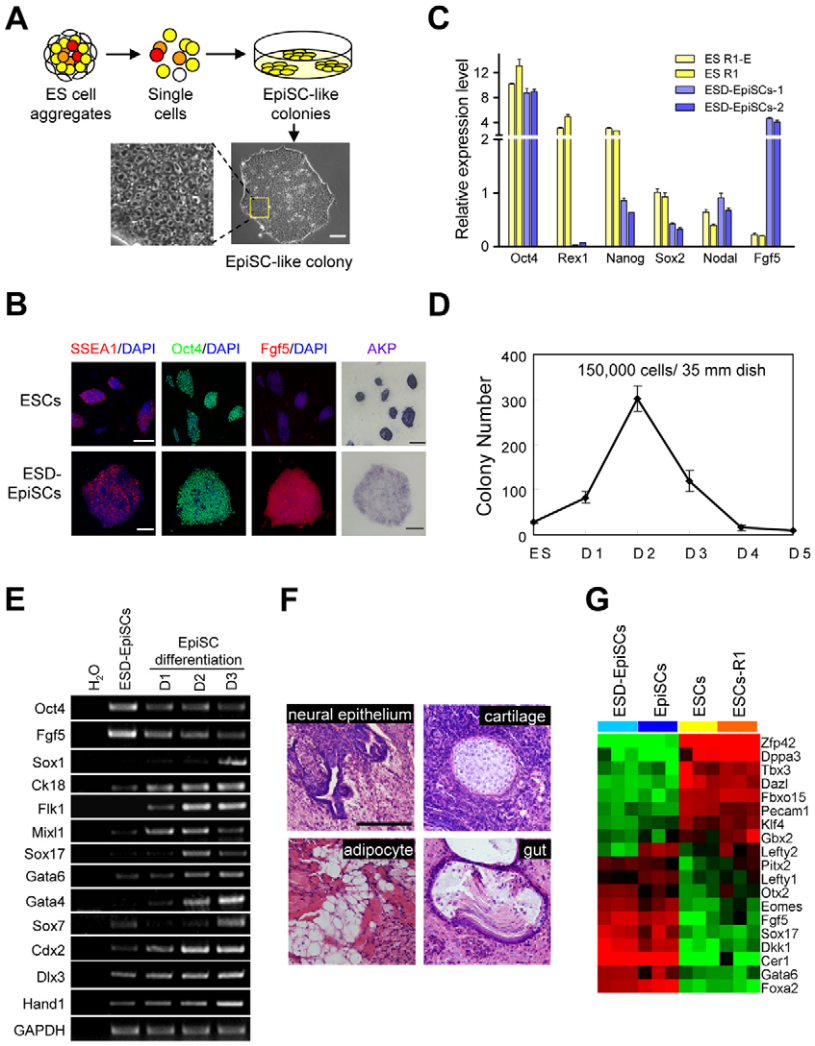

Fig. 4. Cells at the BMP4-sensitive window can be isolated as ESD-EpiSCs. (**A**) Schematic of the method used to derive EpiSC-like colonies from ESC aggregates and the morphology of EpiSC-like colonies. The boxed region is enlarged to show cells with a high nuclear:cytoplasmic ratio. Scale bar: 200 μm. (**B**) Immunostaining for SSEA-1, OCT4 and FGF5 in ESCs and ESD-EpiSCs. Nuclei were stained with DAPI. The enzymatic activity of alkaline phosphatase (AKP) was also analyzed. Scale bar: 100 μm. (**C**) Q-PCR analysis of pluripotency markers in two mouse ESC lines (R1/E and R1) and two ESD-EpiSC lines (ESD-EpiSC-1 was derived from R1/E, and ESD-EpiSC-2 was derived from R1). (**D**) The number of EpiSC-like colonies derived from day 1-5 EBs cultured in KSR medium. On each day, EBs were dissociated into single-cell suspensions, seeded in CDM/AF medium and then the number of colonies counted after 6 days. Undifferentiated ESCs served as a negative control. The seeding density is indicated at the top of the graph. (**E**) Expression of differentiation markers during ESD-EpiSC differentiation in DMEM containing 10% FBS for 3 days. (**F**) Hematoxylin and Eosin histological staining of teratoma sections from ESD-EpiSC-inoculated immunodeficient mice. Neural epithelium, cartilage, adipocytes, and gut epithelium with goblet cells are shown from left to right. Scale bar: 100 μm. (**G**) Microarray gene expression heat map comparing the expression of a selection of genes associated with the ICM or the egg cylinder epiblast in ESD-EpiSCs, EpiSCs, ESCs and ESCs-R1.

to NPCs. A functional study of the role of BMPs in these two stages could help us to better understand their role in these processes. We therefore analyzed the function of BMP4 during the first stage, the transition from ESCs to ESD-EpiSCs. We cultured EBs in KSR medium for 2 days with and without BMP4, and analyzed their gene expression patterns by Q-PCR. BMP4-treated EBs expressed higher levels of *Klf4*, *Rex1* and *Nanog*, but lower levels of *Fgf5*, compared with untreated EBs (Fig. 5A). Immunostaining of FGF5 also showed that BMP4-treatment decreased the number of FGF5-positive cells in day 2 EBs (see Fig. S5A in the supplementary material). Thus, these data suggest that BMP4 inhibits ESC development to the epiblast-like stage. We then further seeded single-cell suspensions of day 2 untreated or BMP4-treated EBs into CDM/AF medium, and the numbers of ESD-EpiSC colonies were counted after 6 days. BMP4 treatment dramatically reduced the number of ESD-EpiSC colonies (Fig. 5B). To analyze whether the decrease in ESD-EpiSC colony number was accompanied by an increase in the number of ESC colonies, we synchronously seeded single-cell suspensions into ESC medium and found that BMP4-treated EBs gave rise to more AKP-positive ESC colonies (see Fig. S5B in the supplementary material). These results suggest that BMP4 inhibits the conversion of ESCs into ESD-EpiSCs.

However, we noticed that BMP4 did not completely inhibit the conversion of ESCs into ESD-EpiSCs (Fig. 5B). To further confirm whether the ESD-EpiSCs derived from BMP4-treated EBs had the same characteristics as those derived from untreated EBs, we examined marker gene expression by Q-PCR. These two types of ESD-EpiSCs expressed comparable levels of *Rex1*, *Klf4*, *Oct4*, *Nodal*, *Nanog* and *Fgf5* (Fig. 5C). Furthermore, we analyzed the differentiation potential of ESD-EpiSCs derived from BMP4-treated EBs and found that they could also differentiate into all three primary germ layers, as well as into trophectoderm (Fig. 5D). These results suggest that the ESD-EpiSCs derived from BMP4-treated EBs are identical to those derived in the absence of BMP4, which supports the notion that the egg cylinder epiblast stage is generic for all germ-layer commitment.

BMP4 suppresses ESD-EpiSC neural commitment and promotes non-neural lineage differentiation

To analyze the function of BMP signaling in the second stage, the transition from ESD-EpiSCs to NPCs, we cultured cell aggregates of ESD-EpiSCs in KSR medium to induce neural differentiation. As detected by immunostaining, 80% of the cells from day 4 ESD-EpiSC aggregates converted to $OCT4^{-}/SOX^{+}$ NPCs (Fig. 6A, control), and BMP4 strongly inhibited this neural conversion (Fig. 6A, BMP4+, 0-4). Furthermore, as detected by Q-PCR, the expression of *Fgf5* and *Oct4* was downregulated and the expression of *Sox1* was upregulated during this process (Fig. 6B). To refine the window of BMP signaling, we added BMP4 to the KSR

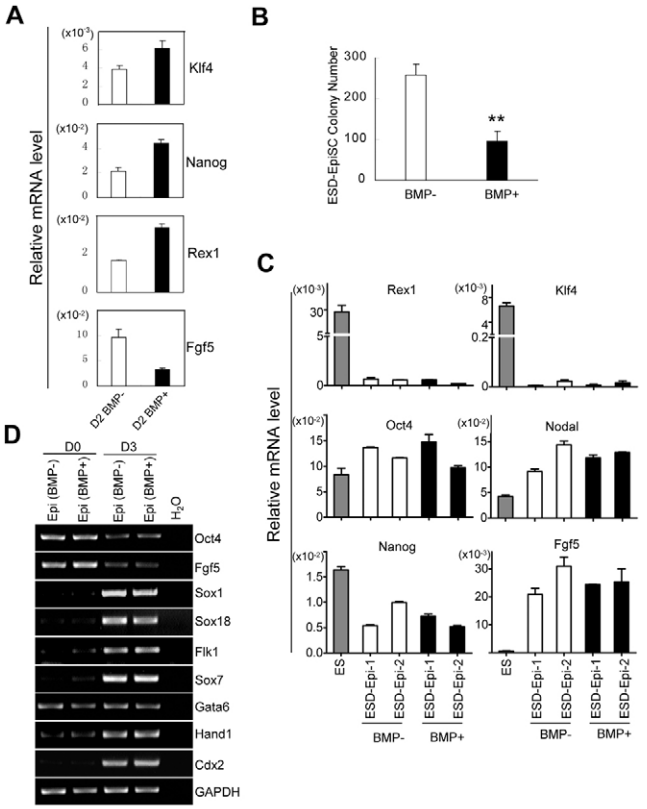

Fig. 5. BMP4 inhibits formation of ESD-EpiSCs from ESCs. (**A**) Q-PCR analysis of *Klf4*, *Nanog*, *Rex1* and *Fgf5* expression in day 2 ESC EBs cultured in KSR medium with or without BMP4 (10 ng/ml). Relative gene expression levels were determined by normalization to the expression of *Gapdh*. (**B**) The number of ESD-EpiSC colonies derived from day 2 EBs cultured in KSR medium with or without BMP4. **, $P<0.01$. (**C**) Q-PCR analysis of *Rex1*, *Klf4*, *Oct4*, *Nodal*, *Nanog* and *Fgf5* expression in ESD-EpiSCs derived from untreated (BMP–) or BMP4-treated (BMP+) day 2 EBs. Two different passages of cells were used for each type of ESD-EpiSC. Undifferentiated ESCs served as the negative control (ES). (**D**) ESD-EpiSCs derived from untreated [Epi (BMP–)] or BMP4-treated [Epi (BMP+)] day 2 EBs were triturated into small clumps and cultured in DMEM containing 10% FBS for 3 days (D3). The expression of germ-layer markers was examined by RT-PCR. Non-induced ESD-EpiSCs served as the negative control (D0).

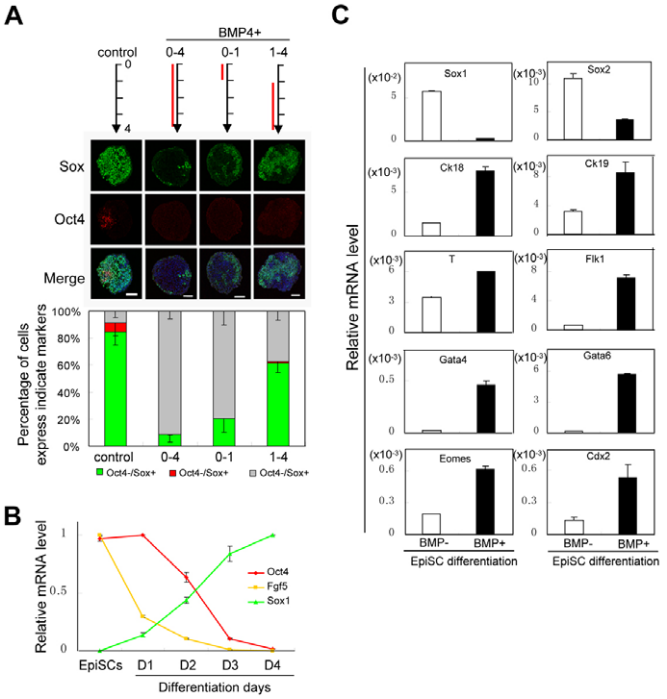

Fig. 6. BMP4 suppresses ESD-EpiSC neural commitment and promotes non-neural lineage differentiation. (**A**) Immunostaining for OCT4 and SOX in ESD-EpiSC aggregates cultured in KSR medium for 4 days. Nuclei were stained with DAPI. BMP4 (10 ng/ml) was added to the medium on the indicated day (red line). The percentage of $OCT4^+/SOX^+$, $OCT4^-/SOX^+$ and $OCT4^-/SOX^-$ cells cultured under the above conditions was obtained from three independent experiments. Scale bar: 50 μm. (**B**) Q-PCR analysis of *Oct4*, *Fgf5* and *Sox1* expression during 4 days of ESD-EpiSC differentiation in KSR medium. (**C**) Q-PCR analysis of germ layer markers in differentiated ESD-EpiSC aggregates cultured for 3 days in the absence or presence of BMP4.

medium at different points and monitored neural differentiation by immunostaining (Fig. 6A). The addition of BMP4 during the first 24 hours effectively reduced the number of $OCT4^-/SOX^+$ NPCs (Fig. 6A, BMP4+, 0-1); however, when BMP4 was present from day 1 to day 4, approximately 60% of the cells still became $OCT4^-/SOX^+$ NPCs (Fig. 6A, BMP4+, 1-4). These results suggest that BMP4 inhibits ESD-EpiSC neural specification at the epiblast stage, which is consistent with the results shown in Fig. 2 and Fig. S2 in the supplementary material. Moreover, in contrast with ESCs, the addition of BMP4 led to reduced OCT4 expression in ESD-EpiSCs (compare Fig. 6A with Fig. 1A), suggesting that BMP4 cannot maintain the pluripotency of ESD-EpiSCs. The addition of BMP4 specifically inhibited the expression of neural markers (*Sox1*, *Sox2*), but promoted the expression of non-neural markers, including epidermal (*Ck18*, *Ck19*), mesodermal (*T*, *Flk1*), endodermal (*Gata4*, *Gata6*) and trophectodermal (*Eomes*, *Cdx2*) markers (Fig. 6C). Collectively, these data indicate that BMP4 inhibits ESD-EpiSC neural commitment and induces ESD-EpiSCs to differentiate into non-neural lineages without maintaining their pluripotency.

Taken together, the above results suggest that BMP4 has distinct functions during ESC neural differentiation. During the first stage, BMP4 inhibits the conversion of ESCs into ESD-EpiSCs, and during the second stage it suppresses ESD-EpiSC neural commitment and promotes non-neural lineage differentiation.

BMP4 inhibits ERK phosphorylation in ESCs, but not in ESD-EpiSCs

The FGF4/ERK pathway has been shown to trigger the transition of pluripotent ESCs from self-renewal to lineage commitment (Kunath et al., 2007; Stavridis et al., 2007; Ying et al., 2008). We consistently found that the addition of FGF4 or bFGF significantly increased the number of ESD-EpiSC colonies derived from day 1 EBs; the number of colonies was comparable to those derived from day 2 EBs (Fig. 7Aa; data not shown). However, the addition of exogenous FGF did not increase the number of ESD-EpiSC colonies derived from day 2 EBs (Fig. 7Aa,C). Given that the highest levels of endogenous *Fgf4* expression were detected in day 1 EBs (Fig. 3A) and the highest number of ESD-EpiSCs was derived from day 2 EBs (Fig. 4D), we proposed that FGF4 might promote ESC differentiation into EpiSCs and that the addition of exogenous FGF might accelerate this process. To determine

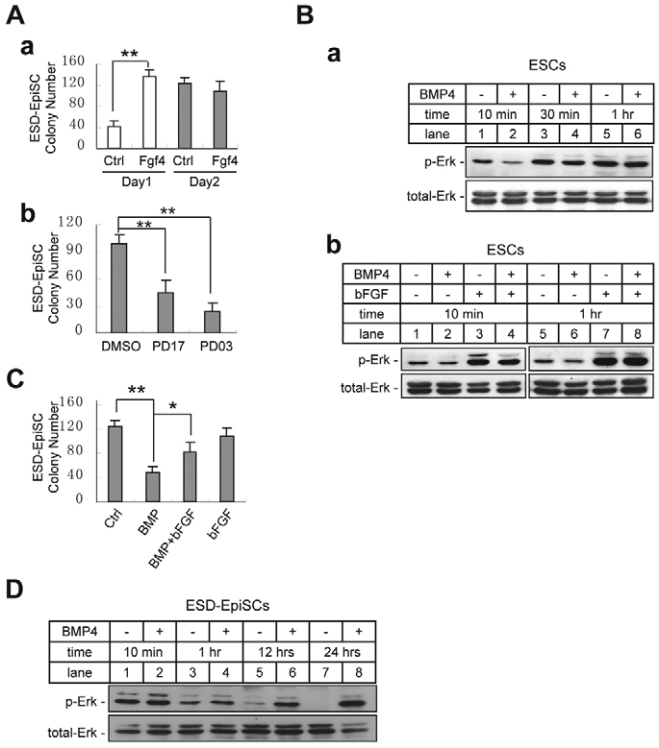

Fig. 7. BMP4 inhibits ERK phosphorylation in ESCs, but not in ESD-EpiSCs. (**A**) The number of ESD-EpiSC colonies derived from day 1 or day 2 EBs cultured in KSR medium with or without FGF4 (5 ng/ml; a). The number of ESD-EpiSC colonies derived from day 2 EBs cultured in KSR medium with DMSO, the FGF receptor inhibitor PD173074 (100 ng/ml) or the MEK inhibitor PD0325901 (1 μM; b). (**B**) ESCs were cultured in standard ES medium without feeder cells, and were washed quickly with KSR medium twice prior to treatment with BMP4 or bFGF. Immunoblot analysis showing ERK phosphorylation in ESCs in response to mock or BMP4 treatment for 10 minutes, 30 minutes, or 1 hour in KSR medium in the absence of LIF (a). Immunoblot analysis showing ERK phosphorylation in ESCs in response to mock treatment or treatment with BMP4 (10 ng/ml), bFGF (5 ng/ml), or BMP4 plus bFGF for 10 minutes or 1 hour in the absence of LIF (b). (**C**) The number of ESD-EpiSC colonies derived from four types of day 2 EBs: mock-treated (control) EBs, or EBs cultured in KSR medium containing BMP4, BMP4 plus bFGF, or bFGF alone. (**D**) Immunoblot analysis showing ERK phosphorylation in ESD-EpiSCs in response to mock treatment or BMP4 treatment for 10 minutes, 1 hour, 12 hours, or 24 hours in KSR medium.

whether the FGF/ERK pathway is involved in BMP4-mediated inhibition during the first stage of ESC differentiation, we cultured ESC EBs for 2 days in the presence of the FGF receptor (FGFR) inhibitor PD173074 (Mohammadi et al., 1998) or the MEK inhibitor PD0325901 (Bain et al., 2007), and found that ESD-EpiSC colony number was dramatically reduced under both conditions (Fig. 7Ab). This effect was similar to that of BMP4 on ESCs (Fig. 5B), and promoted us to determine whether BMP4 inhibited ESC entry into the late epiblast stage via inhibition of the FGF/ERK pathway. Immunoblot analysis showed that BMP4 reduced ERK phosphorylation in ESCs within a short time period (10 minutes) (Fig. 7Ba), which was consistent with results from a previous study (Qi et al., 2004). BMP4 also reduced exogenous FGF-activated ERK phosphorylation in a short time period (Fig. 7Bb, lane 3 versus 4). Moreover, bFGF rescued BMP4-reduced ERK phosphorylation in ESCs (Fig. 7Bb, lane 2 versus 4), and could partially recover the BMP4-induced reduction in ESD-EpiSC colony number (Fig. 7C). Collectively, these data suggest that BMP signaling interferes with the FGF/ERK pathway in the conversion of ESC to ESD-EpiSCs.

We then analyzed whether BMP4 inhibited ERK activity in ESD-EpiSCs. Unexpectedly, BMP4 treatment did not lead to decreased phospho-ERK levels in ESD-EpiSCs (Fig. 7D, lanes 1-4), but instead increased ERK phosphorylation during long-term treatment (Fig. 7D, lanes 5-8). Therefore, BMP4 did not inhibit ERK activity in ESD-EpiSCs. Interestingly, we also found that BMP4 could increase ERK phosphorylation levels in ESCs cultured in N2B27 alone for 24 hours (Ying et al., 2003a) (data not shown), and we speculated that ESCs cultured under such conditions might differentiate into EpiSC-like cells.

IDs partially substituted for BMP4 functions during both stages of ESC neural differentiation

BMP4 was reported to suppress ESC neural differentiation by inducing ID proteins (Ying et al., 2003a). Because ESC neural differentiation could be divided into two stages and BMP4 could induce ID gene expression in both ESCs and EpiSCs (data not shown), we wondered whether ID proteins mediated BMP function at both stages. To address this question, we overexpressed *Id1* and *Id2* in ESCs and ESD-EpiSCs using lentiviral vectors; elevated gene expression was confirmed by Q-PCR (see Fig. S6A-C in the supplementary material). We then cultured the EBs from ID2-ESCs or control-ESCs in KSR medium for 2 days, and found that overexpression of ID2 upregulated *Klf4* and *Rex1* expression and downregulated *Fgf5* expression (Fig. 8A). Immunostaining showed that FGF5 protein levels were reduced in ID2-overexpressing cells (see Fig. S5Ae-h in the supplementary material). ESD-EpiSC colony number assay also showed that overexpression of ID2 significantly inhibited the derivation of ESD-EpiSCs from ESCs (Fig. 8B). Similar to the effect of BMP4, ID2 overexpression did not completely block the derivation of ESD-EpiSCs from ESCs. However, unlike ESD-EpiSCs derived from BMP4-treated EBs (Fig. 5B), ESD-EpiSCs derived from ID2-overexpressing ESCs could not maintained and differentiated after 1-2 passages. We also obtained reproducible results from ID1-overexpressing ESCs (data not shown). Therefore, these data suggest that IDs can partially substitute for the function of BMP4 at the first stage.

We next analyzed the effect of ID2 overexpression on ESD-EpiSC neural differentiation. Unfortunately, the ESD-EpiSCs with high levels of ID2 expression differentiated and could not be maintained as stable cell lines (data not shown); therefore, we could only generate ESD-EpiSCs with low levels of ID2 overexpression. Relative to control ESD-EpiSCs, ID2 overexpression was associated with the downregulation of neuroectoderm marker (*Sox1*, *Sox2*) expression, and the upregulation of mesodermal (*Flk1*, *T*) and trophectodermal (*Cdx2*, *Hand1*) marker expression in day 4 ESD-EpiSC aggregates cultured in KSR medium (Fig. 8C). Similar results were also obtained from ID1-overexpressing ESD-EpiSCs (data not shown). Double immunostaining of SOX and GFP proteins in the day 4 ESD-EpiSC aggregates showed that most of the ID2-overexpressing cells were SOX-negative (Fig. 8Dd-f). Statistical analyses showed that the percentage of SOX^+ and $TUJ1^+$ cells decreased significantly among ID2-overexpressing cells, relative to negative control GFP-expressing cells (Fig. 8D; see also Fig. S6D

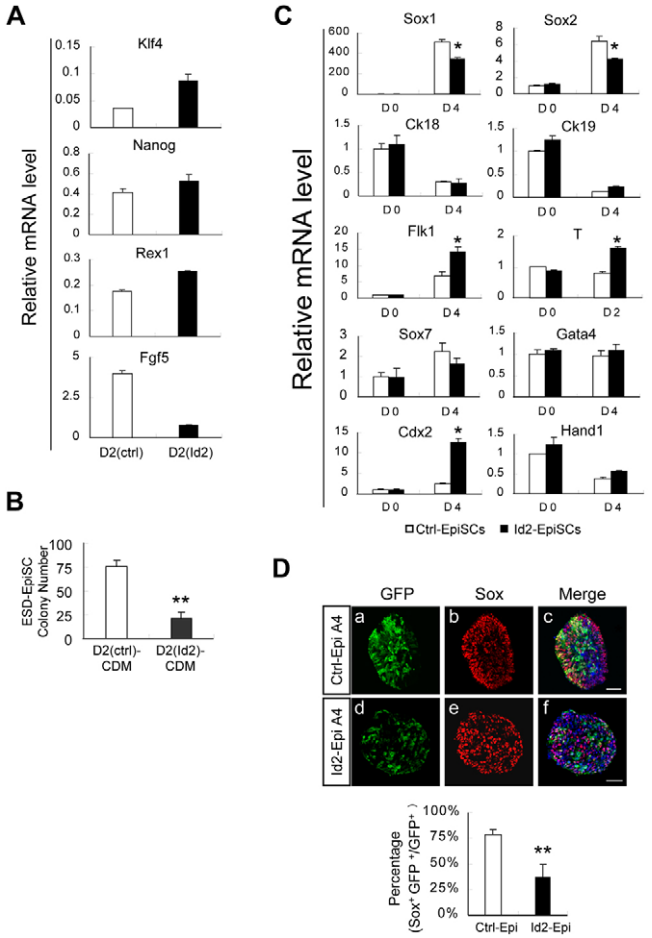

Fig. 8. ID2 partially substituted for BMP4 function at both stages of ESC neural differentiation. (**A**) EBs from control ESCs or ID2-overexpressing ESCs were cultured in KSR medium for 2 days. Expression levels of *Klf4*, *Nanog*, *Rex1* and *Fgf5* were analyzed by Q-PCR and normalized to the expression of *Gapdh*. (**B**) The number of ESD-EpiSCs colonies derived from control ESCs or ID2-overexpressing ESCs. (**C**) Cell aggregates from control ESD-EpiSCs or ID2-overexpressing ESD-EpiSCs were cultured in KSR medium for 4 days. The expression of germ layer markers was analyzed by Q-PCR. (**D**) Immunostaining for GFP (green) and SOX (red) in control or ID2-overexpressing ESD-EpiSC aggregates cultured in KSR medium for 4 days. Nuclei were stained with DAPI (blue). The percentage of SOX^+ cells among GFP^+ cells was obtained from three independent experiments. *, $P<0.05$; **, $P<0.01$. Scale bar: 50 μm.

in the supplementary material), suggesting that ID2 overexpression inhibits ESD-EpiSC neural determination. Taken together, these results suggest that IDs also partially mediate BMP4 function at the second stage of ESC neural differentiation.

DISCUSSION

Although ESCs have been widely used as a model for studying events in early embryogenesis, it remains unclear whether they authentically represent cells in the ICM of peri-implantation blastocysts, or whether they simply represent an artificial state produced in vitro (Niwa, 2007; Silva and Smith, 2008). Importantly, there are no experimental data demonstrating that ESC differentiation definitively passes through an epiblast stage. We show that ESCs pass through an epiblast-like stage during the process of ESC differentiation and can be isolated as EpiSC lines, which have the same characteristics as EpiSCs derived from mouse embryos (Brons et al., 2007; Tesar et al., 2007). Interestingly, we found that the efficiency of ESD-EpiSC derivation was the highest from day 2 EBs (Fig. 4), although these cells can also be derived from undifferentiated ES cells, consistent with recent studies (Guo et al., 2009; Hanna et al., 2009). Therefore, our data provide evidence that ESC differentiation truly passes through an egg-cylinder-epiblast-like stage as part of the early developmental process in vivo. We also show that ESD-EpiSCs derived from the BMP4-treated EBs are identical to those in the absence of BMP4 in terms of marker gene expression and differentiation behavior (Fig. 5). These results suggest that germ layer cell fates have not been decided before the epiblast of egg cylinder stage, and support the notion that the epiblast of egg cylinder stage is generic for all germ-layer commitment. Furthermore, because we can isolate the transition state during ESC neural differentiation and maintain cells as ESD-EpiSCs, we have divided ESC neural differentiation into two stages: the first stage involves the transition from ESCs to EpiSCs, and the second stage involves the transition from EpiSCs to NPCs. These two transitions correspond to the ICM to egg-cylinder-epiblast transition and the egg-cylinder-epiblast to neural ectoderm transition, respectively.

BMP4 has been reported to be required for ESC self-renewal (Kawasaki et al., 2000; Qi et al., 2004; Ying et al., 2003a). Consistently, we show that the addition of BMP4 maintains a portion of $OCT4^+/SOX^+$ pluripotent cells in the ESC EBs (Fig. 1; see also Fig. S1 in the supplementary material). Notably, we also performed a functional assay showing that the addition of BMP4 reduced the number of ESD-EpiSC colonies derived from ESCs (Fig. 5), and that the decreased number of ESD-EpiSC colonies was accompanied by an increase in the number of AKP-positive ESC colonies (see Fig. S5 in the supplementary material), suggesting that BMP4 prevents the conversion of ESCs into ESD-EpiSCs. Moreover, the addition of BMP4 upregulated the expression of ESC markers, whereas it downregulated the expression of epiblast markers in day 2 EBs (Fig. 5; see also Fig. S5 in the supplementary material). On the basis of these data, we suggest that BMP4 maintains ESC pluripotency by preventing the cells from differentiating into late epiblast stage cells, rather than by directly blocking ESC neural commitment (Ying et al., 2003a).

Because the FGF4/ERK pathway primes ESCs to enter the late epiblast-like stage (Kunath et al., 2007; Stavridis et al., 2007; Ying et al., 2008) and BMP4 inhibits MAPK/ERK activity in ESCs (Qi et al., 2004), it is reasonable to propose that BMP4 might inhibit ESC entry into the late epiblast stage by interfering with the FGF/ERK pathway. Indeed, we found that BMP4 reduced both endogenous and exogenous FGF-induced short-term ERK phosphorylation in ESCs (Fig. 7B). Although BMP4 only transiently inhibited ERK phosphorylation, even transient inhibition could be sufficient to change the expression profile of downstream genes of the FGF/ERK signaling pathway (Murphy and Blenis, 2006; Murphy et al., 2002), thereby resulting in changes in ESD-EpiSC formation. We also found that BMP4 did not completely inhibit ERK phosphorylation (Fig. 7B); this incomplete inhibition might explain why BMP4 could not completely block the conversion of ESCs into ESD-EpiSCs (Fig. 5B-D). Cells that escaped BMP4 inhibition might further differentiate into non-neural lineage cells, as we observed in day 6 EBs (Fig. 1B, BMP+). Therefore, BMP4 partially interferes with the FGF/ERK pathway to inhibit the conversion of ESCs to ESD-EpiSCs. Furthermore, we found that IDs, which are downstream

target genes of BMP signaling (Nakashima et al., 2001; Ying et al., 2003a), also inhibited the conversion of ESCs into ESD-EpiSCs (Fig. 8), thus substituting for BMP4 function in the maintenance of ESC pluripotency. Therefore, on the one hand, BMP4 partially interferes with the FGF/ERK pathway and, on the other hand, BMP4 induces ID genes to inhibit ESC entry into the late epiblast stage.

During the second stage of ESC neural differentiation, we noticed that BMP4 could only inhibit the ESD-EpiSC neural differentiation during the first day, and that neural differentiation could not be inhibited once it was under way (Fig. 6). Furthermore, BMP4 maintained approximately half of the ESCs as $OCT4^+/SOX^+$ pluripotent cells (Fig. 1), but could not maintain ESD-EpiSC pluripotency; instead, it promoted the differentiation of these cells into non-neural lineage cells (Fig. 6). Therefore, the egg-cylinder-epiblast-like stage is the critical time point for BMP4 to switch its function from maintaining ESC pluripotency to promoting ESD-EpiSC non-neural differentiation. In contrast to the first stage, BMP4 did not affect ERK activity during the second stage (Fig. 7). Consistent with a previous report that IDs exert a neural lineage-specific blockage on ESC differentiation (Ying et al., 2003a), we found that ID overexpression in ESD-EpiSCs partially inhibited neural differentiation (Fig. 8). We also found that ID overexpression promoted ESD-EpiSCs to differentiate into mesodermal or trophectodermal lineage cells (Fig. 8). Therefore, IDs might partially mediate BMP functions during the second stage of ESC neural differentiation.

Acknowledgements
We thank Dr Austin Smith for providing 46C and TK23 ES cell lines and Dr Anning Lin for critical reading of the manuscript. This work was supported in part by the National Natural Science Foundation of China (30623003, 30721065, 30830034, 90919046), the National Key Basic Research and Development Program of China (2005CB522704, 2006CB943902, 2007CB947101, 2008KR0695 and 2009CB941100), the Shanghai Key Project of Basic Science Research (06DJ14001, 06DZ22032 and 08DJ1400501), and the Council of Shanghai Municipal Government for Science and Technology (088014199).

Competing interests statement
The authors declare no competing financial interests.

Supplementary material
Supplementary material for this article is available at
http://dev.biologists.org/lookup/suppl/doi:10.1242/dev.049494/-/DC1

References

Bain, J., Plater, L., Elliott, M., Shpiro, N., Hastie, C. J., McLauchlan, H., Klevernic, I., Arthur, J. S., Alessi, D. R. and Cohen, P. (2007). The selectivity of protein kinase inhibitors: a further update. *Biochem. J.* **408**, 297-315.
Bibel, M., Richter, J., Schrenk, K., Tucker, K. L., Staiger, V., Korte, M., Goetz, M. and Barde, Y. A. (2004). Differentiation of mouse embryonic stem cells into a defined neuronal lineage. *Nat. Neurosci.* **7**, 1003-1009.
Brons, I. G., Smithers, L. E., Trotter, M. W., Rugg-Gunn, P., Sun, B., Chuva de Sousa Lopes, S. M., Howlett, S. K., Clarkson, A., Ahrlund-Richter, L., Pedersen, R. A. et al. (2007). Derivation of pluripotent epiblast stem cells from mammalian embryos. *Nature* **448**, 191-195.
Brook, F. A. and Gardner, R. L. (1997). The origin and efficient derivation of embryonic stem cells in the mouse. *Proc. Natl. Acad. Sci. USA* **94**, 5709-5712.
Chambers, I., Silva, J., Colby, D., Nichols, J., Nijmeijer, B., Robertson, M., Vrana, J., Jones, K., Grotewold, L. and Smith, A. (2007). Nanog safeguards pluripotency and mediates germline development. *Nature* **450**, 1230-1234.
Coucouvanis, E. and Martin, G. R. (1995). Signals for death and survival: a two-step mechanism for cavitation in the vertebrate embryo. *Cell* **83**, 279-287.
De Robertis, E. M. and Kuroda, H. (2004). Dorsal-ventral patterning and neural induction in Xenopus embryos. *Annu. Rev. Cell Dev. Biol.* **20**, 285-308.
Di-Gregorio, A., Sancho, M., Stuckey, D. W., Crompton, L. A., Godwin, J., Mishina, Y. and Rodriguez, T. A. (2007). BMP signalling inhibits premature neural differentiation in the mouse embryo. *Development* **134**, 3359-3369.
Evans, M. J. and Kaufman, M. H. (1981). Establishment in culture of pluripotential cells from mouse embryos. *Nature* **292**, 154-156.
Gambaro, K., Aberdam, E., Virolle, T., Aberdam, D. and Rouleau, M. (2006). BMP-4 induces a Smad-dependent apoptotic cell death of mouse embryonic stem cell-derived neural precursors. *Cell Death Differ.* **13**, 1075-1087.
Gao, X., Bian, W., Yang, J., Tang, K., Kitani, H., Atsumi, T. and Jing, N. (2001). A role of N-cadherin in neuronal differentiation of embryonic carcinoma P19 cells. *Biochem. Biophys. Res. Commun.* **284**, 1098-1103.
Gardner, R. L. and Rossant, J. (1979). Investigation of the fate of 4-5 day post-coitum mouse inner cell mass cells by blastocyst injection. *J. Embryol. Exp. Morphol.* **52**, 141-152.
Gardner, R. L. and Beddington, R. S. (1988). Multi-lineage 'stem' cells in the mammalian embryo. *J. Cell Sci.* **10**, 11-27.
Guo, G., Yang, J., Nichols, J., Hall, J. S., Eyres, I., Mansfield, W. and Smith, A. (2009). Klf4 reverts developmentally programmed restriction of ground state pluripotency. *Development* **136**, 1063-1069.
Hanna, J., Markoulaki, S., Mitalipova, M., Cheng, A. W., Cassady, J. P., Staerk, J., Carey, B. W., Lengner, C. J., Foreman, R., Love, J. et al. (2009). Metastable pluripotent states in NOD-mouse-derived ESCs. *Cell Stem Cell* **4**, 513-524.
Haub, O. and Goldfarb, M. (1991). Expression of the fibroblast growth factor-5 gene in the mouse embryo. *Development* **112**, 397-406.
Hayashi, K., Lopes, S. M., Tang, F. and Surani, M. A. (2008). Dynamic equilibrium and heterogeneity of mouse pluripotent stem cells with distinct functional and epigenetic states. *Cell Stem Cell* **3**, 391-401.
Hemmati-Brivanlou, A. and Melton, D. (1997a). Vertebrate embryonic cells will become nerve cells unless told otherwise. *Cell* **88**, 13-17.
Hemmati-Brivanlou, A. and Melton, D. (1997b). Vertebrate neural induction. *Annu. Rev. Neurosci.* **20**, 43-60.
Kawasaki, H., Mizuseki, K., Nishikawa, S., Kaneko, S., Kuwana, Y., Nakanishi, S., Nishikawa, S. I. and Sasai, Y. (2000). Induction of midbrain dopaminergic neurons from ES cells by stromal cell-derived inducing activity. *Neuron* **28**, 31-40.
Khokha, M. K., Yeh, J., Grammer, T. C. and Harland, R. M. (2005). Depletion of three BMP antagonists from Spemann's organizer leads to a catastrophic loss of dorsal structures. *Dev. Cell* **8**, 401-411.
Kunath, T., Saba-El-Leil, M. K., Almousailleakh, M., Wray, J., Meloche, S. and Smith, A. (2007). FGF stimulation of the Erk1/2 signalling cascade triggers transition of pluripotent embryonic stem cells from self-renewal to lineage commitment. *Development* **134**, 2895-2902.
Lendahl, U., Zimmerman, L. B. and McKay, R. D. (1990). CNS stem cells express a new class of intermediate filament protein. *Cell* **60**, 585-595.
Linker, C. and Stern, C. D. (2004). Neural induction requires BMP inhibition only as a late step, and involves signals other than FGF and Wnt antagonists. *Development* **131**, 5671-5681.
Lu, C. C., Brennan, J. and Robertson, E. J. (2001). From fertilization to gastrulation: axis formation in the mouse embryo. *Curr. Opin. Genet. Dev.* **11**, 384-392.
Martin, G. R. (1981). Isolation of a pluripotent cell line from early mouse embryos cultured in medium conditioned by teratocarcinoma stem cells. *Proc. Natl. Acad. Sci. USA* **78**, 7634-7638.
Mohammadi, M., Froum, S., Hamby, J. M., Schroeder, M. C., Panek, R. L., Lu, G. H., Eliseenkova, A. V., Green, D., Schlessinger, J. and Hubbard, S. R. (1998). Crystal structure of an angiogenesis inhibitor bound to the FGF receptor tyrosine kinase domain. *EMBO J.* **17**, 5896-5904.
Murphy, L. O. and Blenis, J. (2006). MAPK signal specificity: the right place at the right time. *Trends Biochem. Sci.* **31**, 268-275.
Murphy, L. O., Smith, S., Chen, R. H., Fingar, D. C. and Blenis, J. (2002). Molecular interpretation of ERK signal duration by immediate early gene products. *Nat. Cell. Biol.* **4**, 556-564.
Nakashima, K., Takizawa, T., Ochiai, W., Yanagisawa, M., Hisatsune, T., Nakafuku, M., Miyazono, K., Kishimoto, T., Kageyama, R. and Taga, T. (2001). BMP2-mediated alteration in the developmental pathway of fetal mouse brain cells from neurogenesis to astrocytogenesis. *Proc. Natl. Acad. Sci. USA* **98**, 5868-5873.
Naldini, L., Blomer, U., Gage, F. H., Trono, D. and Verma, I. M. (1996). Efficient transfer, integration, and sustained long-term expression of the transgene in adult rat brains injected with a lentiviral vector. *Proc. Natl. Acad. Sci. USA* **93**, 11382-11388.
Nichols, J., Zevnik, B., Anastassiadis, K., Niwa, H., Klewe-Nebenius, D., Chambers, I., Scholer, H. and Smith, A. (1998). Formation of pluripotent stem cells in the mammalian embryo depends on the POU transcription factor Oct4. *Cell* **95**, 379-391.
Niwa, H. (2007). How is pluripotency determined and maintained? *Development* **134**, 635-646.
Okada, Y., Shimazaki, T., Sobue, G. and Okano, H. (2004). Retinoic-acid-concentration-dependent acquisition of neural cell identity during in vitro differentiation of mouse embryonic stem cells. *Dev. Biol.* **275**, 124-142.
Oliver, G., Mailhos, A., Wehr, R., Copeland, N. G., Jenkins, N. A. and Gruss, P. (1995). Six3, a murine homologue of the sine oculis gene, demarcates the most anterior border of the developing neural plate and is expressed during eye development. *Development* **121**, 4045-4055.

Pelton, T. A., Sharma, S., Schulz, T. C., Rathjen, J. and Rathjen, P. D. (2002). Transient pluripotent cell populations during primitive ectoderm formation: correlation of in vivo and in vitro pluripotent cell development. *J. Cell Sci.* **115**, 329-339.
Peng, G., Han, M., Du, Y., Lin, A., Yu, L., Zhang, Y. and Jing, N. (2009). SIP30 is regulated by ERK in peripheral nerve injury-induced neuropathic pain. *J. Biol. Chem.* **284**, 30138-30147.
Pevny, L. H., Sockanathan, S., Placzek, M. and Lovell-Badge, R. (1998). A role for SOX1 in neural determination. *Development* **125**, 1967-1978.
Pfister, S., Steiner, K. A. and Tam, P. P. (2007). Gene expression pattern and progression of embryogenesis in the immediate post-implantation period of mouse development. *Gene Expr. Patterns* **7**, 558-573.
Qi, X., Li, T. G., Hao, J., Hu, J., Wang, J., Simmons, H., Miura, S., Mishina, Y. and Zhao, G. Q. (2004). BMP4 supports self-renewal of embryonic stem cells by inhibiting mitogen-activated protein kinase pathways. *Proc. Natl. Acad. Sci. USA* **101**, 6027-6032.
Rathjen, J., Lake, J. A., Bettess, M. D., Washington, J. M., Chapman, G. and Rathjen, P. D. (1999). Formation of a primitive ectoderm like cell population, EPL cells, from ES cells in response to biologically derived factors. *J. Cell Sci.* **112**, 601-612.
Reversade, B. and De Robertis, E. M. (2005). Regulation of ADMP and BMP2/4/7 at opposite embryonic poles generates a self-regulating morphogenetic field. *Cell* **123**, 1147-1160.
Rivera-Perez, J. A. and Magnuson, T. (2005). Primitive streak formation in mice is preceded by localized activation of Brachyury and Wnt3. *Dev. Biol.* **288**, 363-371.
Rogers, M. B., Hosler, B. A. and Gudas, L. J. (1991). Specific expression of a retinoic acid-regulated, zinc-finger gene, Rex-1, in preimplantation embryos, trophoblast and spermatocytes. *Development* **113**, 815-824.
Rosner, M. H., Vigano, M. A., Ozato, K., Timmons, P. M., Poirier, F., Rigby, P. W. and Staudt, L. M. (1990). A POU-domain transcription factor in early stem cells and germ cells of the mammalian embryo. *Nature* **345**, 686-692.
Rossant, J. (2008). Stem cells and early lineage development. *Cell* **132**, 527-531.
Sasal, Y., Lu, B., Steinbelsser, H. and De Robertis, E. M. (1995). Regulation of neural induction by the Chd and Bmp-4 antagonistic patterning signals in Xenopus. *Nature* **378**, 419.
Shi, Y. and Massague, J. (2003). Mechanisms of TGF-beta signaling from cell membrane to the nucleus. *Cell* **113**, 685-700.
Silva, J. and Smith, A. (2008). Capturing pluripotency. *Cell* **132**, 532-536.
Snow, M. H. L. (1977). Gastrulation in the mouse: growth and regionalization of the epiblast. *J. Embryol. Exp. Morphol.* **42**, 293-303.
Stavridis, M. P., Lunn, J. S., Collins, B. J. and Storey, K. G. (2007). A discrete period of FGF-induced Erk1/2 signalling is required for vertebrate neural specification. *Development* **134**, 2889-2894.
Tam, P. P. and Loebel, D. A. (2007). Gene function in mouse embryogenesis: get set for gastrulation. *Nat. Rev. Genet.* **8**, 368-381.
Tanaka, S., Kamachi, Y., Tanouchi, A., Hamada, H., Jing, N. and Kondoh, H. (2004). Interplay of SOX and POU factors in regulation of the Nestin gene in neural primordial cells. *Mol. Cell. Biol.* **24**, 8834-8846.
Tesar, P. J., Chenoweth, J. G., Brook, F. A., Davies, T. J., Evans, E. P., Mack, D. L., Gardner, R. L. and McKay, R. D. (2007). New cell lines from mouse epiblast share defining features with human embryonic stem cells. *Nature* **448**, 196-199.
Thomas, P. and Beddington, R. (1996). Anterior primitive endoderm may be responsible for patterning the anterior neural plate in the mouse embryo. *Curr. Biol.* **6**, 1487-1496.
Tiscornia, G., Singer, O. and Verma, I. M. (2006). Production and purification of lentiviral vectors. *Nat. Protoc.* **1**, 241-245.
Toyooka, Y., Shimosato, D., Murakami, K., Takahashi, K. and Niwa, H. (2008). Identification and characterization of subpopulations in undifferentiated ES cell culture. *Development* **135**, 909-918.
Tropepe, V., Hitoshi, S., Sirard, C., Mak, T. W., Rossant, J. and van der Kooy, D. (2001). Direct neural fate specification from embryonic stem cells: a primitive mammalian neural stem cell stage acquired through a default mechanism. *Neuron* **30**, 65-78.
Watanabe, K., Kamiya, D., Nishiyama, A., Katayama, T., Nozaki, S., Kawasaki, H., Watanabe, Y., Mizuseki, K. and Sasai, Y. (2005). Directed differentiation of telencephalic precursors from embryonic stem cells. *Nat. Neurosci.* **8**, 288-296.
Wilson, P. A. and Hemmati-Brivanlou, A. (1995). Induction of epidermis and inhibition of neural fate by Bmp-4. *Nature* **376**, 331-333.
Wilson, S. I. and Edlund, T. (2001). Neural induction: toward a unifying mechanism. *Nat. Neurosci.* **4**, 1161-1168.
Wood, H. B. and Episkopou, V. (1999). Comparative expression of the mouse Sox1, Sox2 and Sox3 genes from pre-gastrulation to early somite stages. *Mech. Dev.* **86**, 197-201.
Xia, C., Wang, C., Zhang, K., Qian, C. and Jing, N. (2007). Induction of a high population of neural stem cells with anterior neuroectoderm characters from epiblast-like P19 embryonic carcinoma cells. *Differentiation* **75**, 912-927.
Ying, Q. L., Nichols, J., Chambers, I. and Smith, A. (2003a). BMP induction of Id proteins suppresses differentiation and sustains embryonic stem cell self-renewal in collaboration with STAT3. *Cell* **115**, 281-292.
Ying, Q. L., Stavridis, M., Griffiths, D., Li, M. and Smith, A. (2003b). Conversion of embryonic stem cells into neuroectodermal precursors in adherent monoculture. *Nat. Biotechnol.* **21**, 183-186.
Ying, Q. L., Wray, J., Nichols, J., Batlle-Morera, L., Doble, B., Woodgett, J., Cohen, P. and Smith, A. (2008). The ground state of embryonic stem cell self-renewal. *Nature* **453**, 519-523.

Table S1. Primer sequences (5′→3′) for Q-PCR and RT-PCR

Genes	5′ Primer	3′ Primer
Rex1	CAGTTCGTCCATCTAAAAAGGGAGG	TCTTAGCTGCTTCCTTGAACAATGCC
Oct4	AGTTGGCGTGGAGACTTTGC	CAGGGCTTTCATGTCCTGG
Nanog	TTGCTTACAAGGGTCTGCTACT	ACTGGTAGAAGAATCAGGGCT
Nodal	CCTGGAGCGCATTTGGATG	ACTTTTCTGCTCGACTGGACA
Fgf5	GCTGTGTCTCAGGGGATTGT	CACTCTCGGCCTGTCTTTTC
Sox2	GCGGAGTGGAAACTTTTGTCC	CGGGAAGCGTGTACTTATCCTT
Sox1	GCACACAGCGTTTTCTCGG	ACATCCGACTCCTCTTCCC
Ck18	CAGCCAGCGTCTATGCAGG	CTTTCTCGGTCTGGATTCCAC
Ck19	GGGGGTTCAGTACGCATTGG	GAGGACGAGGTCACGAAGC
T (brachyury)	CTCGGATTCACATCGTGAGAG	AAGGCTTTAGCAAATGGGTTGTA
Flk1	GGGTCGATTTCAAACCTCAATGT	AGAGTAAAGCCTATCTCGCTGT
Sox17	CGAGCCAAAGCGGAGTCTC	TGCCAAGGTCAACGCCTTC
Gata6	TTGCTCCGGTAACAGCAGTG	GTGGTCGCTTGTGTAGAAGGA
Gata4	CCCTACCCAGCCTACATGG	ACATATCGAGATTGGGGTGTCT
Eomes	CCTGGTGGTGTTTTGTTGTG	TTTAATAGCACCGGGCACTC
Cdx2	GCTACGGCGAACTTGGACA	GTGATGGTGCGCGTGGTAT
Sox7	ATGCTGGGAAAGTCATGGAAG	CGTGTTCTGGTCACGAGAGA
Klf4	CTTCAGCTATCCGATCCGGG	GAGGGGCTCACGTCATTGAT
Tbx3	GAACCTACCTGTTCCCGGAAA	CAATGCCCAATGTCTCGAAAAC
Acvr2b	ACCCCCAGGTGTACTTCTG	CATGGCCGTAGGGAGGTTTC
Gbx2	GCAAGGGAAAGACGAGTCAAA	GGCAAATTGTCATCTGAGCTGTA
Foxa2	TAGCGGAGGCAAGAAGACC	CTTAGGCCACCTCGCTTGT
Pitx2	GCAGCCGTTGAATGTCTCTTC	GTCCGTGAACTCGACCTTTTT
Cer1	CTCTGGGGAAGGCAGACCTAT	CCACAAACAGATCCGGCTT
Fgf4	GGGCATCGGATTCCACCTG	GCTGCTCATAGCCACGAAGAA
Six3	CCGGAAGAGTTGTCCATGTTC	CGACTCGTGTTTGTTGATGGC
Hesx1	CCGCTTTCACCCAGAACCA	ATCTTTGCTCGGCGATTTTGG
Pax6	GCAGATGCAAAAGTCCAGGTG	CAGGTTGCGAAGAACTCTGTTT